Analyst

PAPER

View Article Online
View Journal | View Issue

Cite this: *Analyst*, 2017, **142**, 1619

In situ quantification and evaluation of ClO^-/H_2S homeostasis in inflammatory gastric tissue by applying a rationally designed dual-response fluorescence probe featuring a novel H^+-activated mechanism†

Qiang Fu,‡[a,b] Guang Chen,*‡[a,c] Yuxia Liu,[a] Ziping Cao,[a] Xianen Zhao,[a] Guoliang Li,[a] Fabiao Yu,[c] Lingxin Chen,[c] Hua Wang*[a] and Jinmao You*[a,b]

Homeostasis of ClO^-/H_2S plays a crucial role in the damage and repair of gastric tissue, but has rarely been investigated due to the challenge of *in situ* analysis in the highly acidic gastric environment. Herein, we designed a new H^+-activated optical mechanism, involving controllable photoinduced electron transfer (PET) and switch of electron push–pull (SEPP), to develop the simple yet multifunctional probe (*Z*)-4-(2-benzylidenehydrazinyl)-7-nitrobenzo[*c*][1,2,5]oxadiazole (BNBD). First, the BNBD probe (Off) was protonated by the highly acidic media to trigger strong fluorescence (On). Then, the analytes ClO^- and H_2S reacted with the protonated BNBD, leading to ultrasensitive (ClO^-: 2.7 nM and H_2S: 6.9 nM) fluorescence quenching *via* the rapid oxidation of C=N (50 s) and nitro reduction (10 s), respectively. With the logical discrimination by absorbance/colour (ClO^-: 300 nm/colorless and H_2S: 400 nm/orange), a strategy for the *in situ* quantification of ClO^-/H_2S in gastric mucosa and juice was developed. For the first time, the *in situ* quantitative monitoring of endogenous H_2S and ClO^-/H_2S homeostasis as well as the pathologic manifestation in gastric mucosa were realized, thus overcoming the challenge of ClO^-/H_2S analysis under highly acidic conditions and enabling the *in situ* tissue quantification of ClO^-/H_2S. In combination with the assessment of mucosal damage, this study confirms the injurious/rehabilitative effects of ClO^-/H_2S on gastric mucosa (at 50–90 μm depth), which may facilitate the auxiliary diagnosis of stomach diseases induced by oxidative stress.

Received 10th February 2017,
Accepted 22nd March 2017

DOI: 10.1039/c7an00244k

rsc.li/analyst

Introduction

The redox balance between reactive oxygen species (ROS) and reductive sulphur species (RSS) plays a vital role in biological processes such as cell proliferation, differentiation, and apoptosis.[1] The imbalance caused by the overproduction of ROS overwhelms the defence mechanism in animals and induces serious consequences such as peroxidation, DNA damage, and even carcinogenesis.[2] Hydrogen sulfide (H_2S) has always been proven to be anti-apoptotic and anti-inflammatory.[3] More recently, H_2S has been demonstrated to have curative effects on gastric mucosa. Novel drugs that can release H_2S in gastric juice and tissue have been designed for the treatment of ulcerative, inflammatory, and malignant tumour diseases in the gastrointestinal tract.[4,5] However, more and more people and even domestic animals suffer from gastritis, which is inflammation of gastric mucosa.[6] One important reason for this lies in the fact that the excessive hypochlorite (ClO^-)[7] daily ingested from water can consume H_2S in the stomach through a fast reaction.[8] As a long-term consequence of oxidative injury, the stomach lining becomes inflamed, ulcerated,[9] and finally even cancerous at the site of the inflammatory tissue *via* the metaplasia process.[10] Even worse, the increased chlorine level is associated with the severity of atrophic gastritis, which is a type of gastritis that has the highest probability to become cancerous.[6] Therefore, it is

[a]*The Key Laboratory of Life-Organic Analysis, Key Laboratory of Pharmaceutical Intermediates and Analysis of Natural Medicine, Qufu Normal University, Qufu 273165, Shandong, China. E-mail: chenandguang@163.com, huawangqfnu@126.com, jmyou6304@163.com*
[b]*Qinghai Normal University, Xining, China*
[c]*Key Laboratory of Coastal Environmental Processes and Ecological Remediation, The Research Centre for Coastal Environmental Engineering and Technology, Yantai Institute of Coastal Zone Research, Chinese Academy of Sciences, Yantai 264003, China*

†Electronic supplementary information (ESI) available. See DOI: 10.1039/c7an00244k

‡These authors contributed equally to the present work.

urgently necessary to perform research on ClO^-/H_2S homeostasis in the gastric environment. Particularly, in the current treatment of chronic stomach disease, physicians have to prescribe a large number of various drugs to patients. The most important reason for this lies in the fact that various gastritis always lead to similar symptoms; therefore, the specific pathogenesis cannot be understood. If gastritis or ulcer can be determined as an injury that is the result of oxidative stress, the therapeutic plan will become more efficient.[11]

Traditionally, the detection of ClO^- or H_2S in tissue requires complex procedures involving sample pretreatment and analyte separation and enrichment.[11] However for pathological studies, *in situ* detection is more significant in practice owing to its high accuracy, reliability, and convenience. However, due to the lack of novel techniques, *in situ* tissue quantification is still a challenge. In recent years, fluorescence imaging technique based on chemical probes makes *in situ* tissue quantification possible,[12] a precondition of which is the need to design a rapid and sensitive probe for the target. Many excellent chemical probes have been devised to monitor ROS molecules, such as ClO^-, in various biological samples.[13–18] Moreover, many elaborate probes have also been designed for the quantification of RSS in blood, tissues, cells, and organelles.[19–26] In addition, to explore oxidative stress, some excellent dual-response probes have been designed, with which redox pairs, such as superoxide anion/hydrogen polysulfide, peroxynitrite/glutathione,[27–29] hydrogen peroxide/hydrogen sulfides,[30] and hypobromous acid/hydrogen sulfide,[31] can be detected in biological samples. However, dual-response fluorescence probes for ClO^-/H_2S are rather scarce. Except for an excellent probe for cell research,[32] no probe is available for the pair of ClO^-/H_2S. Furthermore, since the gastric environment in the fasting state (medical condition: empty stomach) is always highly acidic, a dual-response probe capable of detecting ClO^-/H_2S in the presence of H^+ is highly required. To the best of our knowledge, there is no report yet describing such a probe and application for the study of ClO^-/H_2S homeostasis in stomach samples.

Herein, we designed a rapid, sensitive, and selective dual-response fluorescent probe capable of *in situ* quantification of ClO^-/H_2S in gastric tissue. Usually, the fluorescence response triggered by the cleavage of the C=N bond in a fluorophore can be used to detect ClO^-.[33] Accordingly, we hypothesized that combining an electron-rich group with C=N might accelerate the oxidation of C=N by oxidative ClO^-. Thus, a phenyl–C=N–N–R group was designed as a fast reporter group for ClO^-. On the other hand, *in situ* determination of endogenous H_2S in tissue is still a challenge because it requires a rapid and sensitive response. It was found that sensing H_2S through nucleophilic attack or CuS precipitation needs a relatively long time.[34] Although azide in the fluorophore could rapidly detect trace levels of H_2S within minutes, it might get protonated in the highly acidic environment. In contrast, the nitro reduction[35] by H_2S was thought to be the best choice for this study. With these speculations in mind, we searched for appropriate fluorophores that could be easily equipped with the abovementioned reporting groups and more importantly, could help accomplish a rapid and sensitive response towards ClO^-/H_2S under highly acidic conditions. 4-Nitrobenzo-2-oxa-1,3-diazole (NBD) was demonstrated to be advantageous in terms of long-wavelength absorption/emission, high quantum yield, good cell permeability, and low toxicity.[36] According to

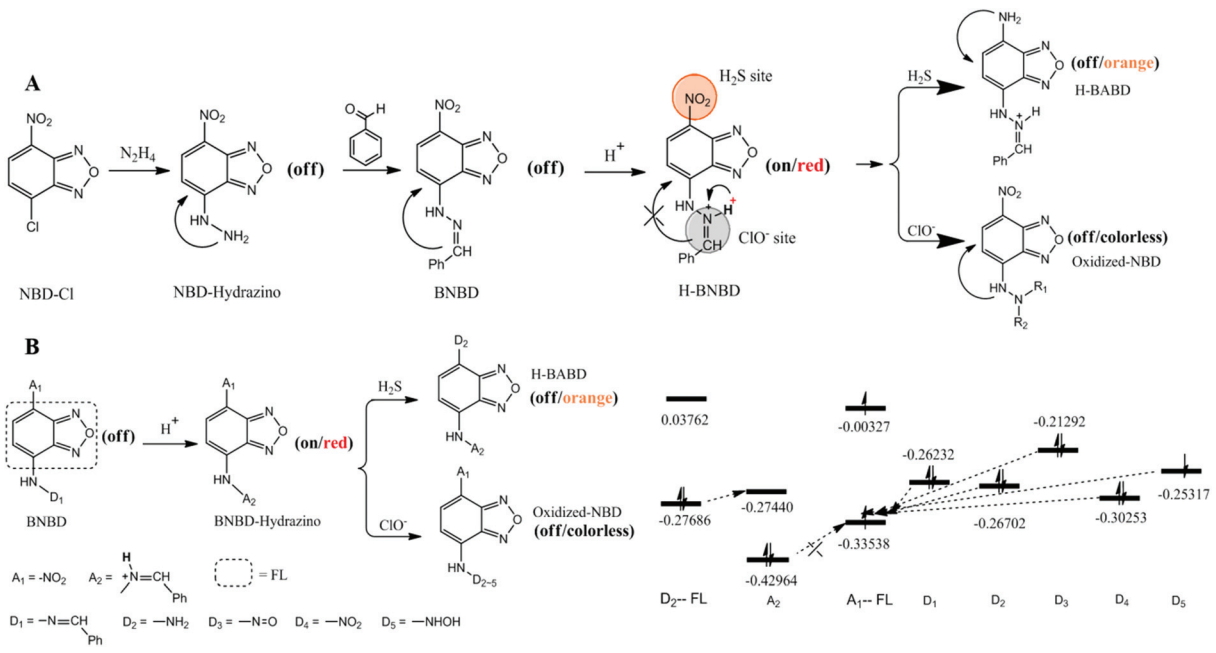

Scheme 1 Design of the BNBD probe *via* the H^+-activated mechanism (A) and the proposed products with the estimated orbital energy (B) *via* density functional theory (DFT) at the B3LYP level with the standard 6-31g(d,p) basis set (note: the unit for energy is Hartree).

our study, a hydrazino group in the 7-position of NBD (NBD-Hydrazino) will contribute to photoinduced electron transfer (PET). Based on this mechanism (Scheme 1), we further envisioned that a phenyl–C=N–N–R group attached to the NBD molecule would result in more efficient PET with its rich π electrons (high-energy). Interestingly, nitrogen in C=N holds the potential to be protonated by H^+, which possibly leads to the stable conjugated phenyl–C=N^+–H (H-BNBD). Thus, PET would be inhibited and thereby strong fluorescence would be triggered. Upon reaction with ClO^- or H_2S, the strong fluorescence of H-NBD would be rapidly quenched in return. More interestingly, the corresponding two products have the opposite electron push–pull and would provide different absorbances (or colours) that could enable differentiation between ClO^- and H_2S. Therefore, this design would provide a rapid, sensitive, and selective dual-response fluorescent probe for us to achieve the aim of *in situ* ClO^-/H_2S quantification in acidic gastric tissue.

In the present study, a new dual-response probe, (*Z*)-4-(2-benzylidenehydrazinyl)-7-nitrobenzo[*c*][1,2,5]oxadiazole (BNBD), which works using a novel H^+-activated sensing mechanism, was developed and applied to the *in situ* quantitative monitoring of ClO^-/H_2S homeostasis in gastric mucosa and juice. BNBD provides rapid (within sec) UV absorbance and fluorescence responses, allowing for the logical discrimination and quantitation of ClO^-/H_2S. The H^+-activated Off–On–Off switch of BNBD provides the ultrasensitive (nM) detection of ClO^-/H_2S. Satisfactory selectivity to ClO^-/H_2S over other analogues of ROS and RSS, as well as substances coexisting in the stomach was achieved. For the first time, endogenous H_2S and the homeostasis of ClO^-/H_2S in stomach tissue were quantitatively monitored *via* fluorescence imaging. Moreover, the rehabilitative effect of endogenous H_2S on ClO^--caused mucosa injury was explored based on the homeostasis of ClO^-/H_2S. The results associate the ClO^-/H_2S homeostasis with the pathologic manifestation in gastric mucosa, which is expected to serve as a significant reference for the diagnosis and therapy of stomach diseases.

Experimental

Synthesis of BNBD probe

To 50 mL of chloroform containing 0.30 g of NBD-Cl (7-chloro-4-nitrobenzo-2-oxa-1,3-diazole), 50 mL of methanol solution of hydrazine hydrate (0.3 mL) was added. The mixture was stirred at ambient temperature for 30 min, producing a brown precipitate which was then washed with ethyl acetate (0.29 g, yield: 97%) and named as NBD-Hydrazino. Then, an aliquot of 1.0 mmol of NBD-Hydrazino (0.195 g) was transferred to 20 mL of ethanol, to which 1.5 mmol of benzaldehyde (0.16) and 0.1 mL of glacial acetic acid were sequentially added. The obtained mixture was stirred and heated at reflux temperature for 3 h. Then, the red precipitate was purified by flash column chromatography (ethyl acetate/petroleum ether: 1/1), yielding 0.245 g of red powder (86%), named as BNBD, which was stored in a refrigerator at 4 °C when not in use. The ^1H NMR, ^{13}C NMR, and MS spectra are illustrated in Fig. S1–3.†

Preparation of the test solutions

The stock solution of the BNBD probe was prepared at 1.0×10^{-4} M in ACN. Stock solutions of Na_2S and ClO^- were prepared at 1.0×10^{-3} M in distilled water. Solutions for other testing species including Cu^{2+}, Fe^{3+}, Zn^{2+}, Co^{2+}, Ca^{2+}, F^-, SO_4^{2-}, HCO_3^-, NO_2^-, NO_3^-, SO_3^{2-}, Cl^-, PO_4^{3-}, I^-, Mg^{2+}, $O_2^{\bullet-}$, H_2O_2, $OH^{\bullet}$, $ONOO^-$, HSO_3^-, SO_3^{2-}, $S_2O_3^-$, $S_2O_4^{2-}$, $S_2O_5^{2-}$, SCN^-, NO, Cl^-, Br^-, I^-, N_3^-, SO_4^{2-}, HPO_4^{2-}, OAc^-, citrate, lipoic acid, metallothionein, glutathione, cysteine, and *S*-nitrosoglutathione were prepared in twice-distilled water according to the reported methods.[37–40] A solution of the BNBD probe (3 μM) was prepared by mixing 30 μL of probe stock solution with 670 μL of Britton-Robinson buffer (aqueous, pH 1.98), 200 μL distilled water, and 100 μL of ACN in 1 mL solution (pH 1.98). The test solutions of the BNBD probe were prepared by mixing 0–200 μL of Na_2S/ClO^- stock solution, 30 μL of BNBD probe solution, 670 μL of Britton-Robinson buffer (aqueous, pH 1.98), 0–200 μL distilled water, and 100 μL of ACN in 1 mL solution (pH 1.98). The resulting solutions were stirred and allowed to stand for 60 min at 37 °C before obtaining their spectra.

Solutions of simulated/real gastric juice

Simulated gastric juice was prepared by diluting 0.2 g of NaCl, 0.32 g of pepsin, and 0.7 mL of concentrated hydrochloric acid (HCl) to 100 mL pure water and the pH was adjusted to 1.98 using concentrated HCl.[41] Real gastric juice was obtained from a rabbit in the morning after fasting overnight *via* a home-made gastric tube. Blank solutions of ClO^- and H_2S were obtained by fluorescence titration experiments with Na_2S and ClO^-, respectively. The test solutions of the simulated/real gastric juice were prepared by mixing 30 μL of BNBD probe solution, 100 μL of simulated/real gastric juice, 670 μL of Britton-Robinson buffer (aqueous, pH 1.98), 100 μL distilled water, and 100 μL of ACN in 1 mL solution (pH 1.98). (Note: the volume of BR buffer was sufficient to maintain the final pH as 1.98 although pH of real gastric juice fluctuates within a certain range.)

Gastric mucosa imaging

The gastric mucosa was scraped off, washed by artificial gastric fluid, and then pressed into a thin layer of about 1 mm. The obtained gastric mucosa was incubated with a solution (1.0 mL, pH 1.98) consisting of 30 μL of BNBD stock solution, 100 μL of artificial/real gastric juice, 670 μL of Britton-Robinson buffer (aqueous), 100 μL distilled water, and 100 μL of ACN. After 15 min, the tissue was scanned by confocal microscopy using the excitation wavelength of 488 nm and investigated over the wavelengths of 500–600 nm.

All animals were treated following the guidelines approved by the Institutional Animal Care and Use Committee of the National Health Research Institutes.

Calibration curves of ClO^-/H_2S in gastric mucosa

Accurate calibration for analytes in tissue with fluorescence imaging is still a challenge. Pioneering work provided the method to establish the calibration curve for the target in universal buffer solution.[12] In this study, we used the target in gastric juice instead as an improvement to establish the calibration curve based on the permeability of the gastric mucosa for acid and some other substances.[42] Thus, the calibration curve of fluorescence intensities (*Y*) *versus* target in gastric juice (*X*) was established to achieve more accurate quantification in mucosal tissue. To obtain the average value with a stable signal, fluorescence intensities were obtained from the 5 *xy* planes at the same depths with replicate experiments (n = 5). For each site, a total of 25 intensities were obtained along the *z*-direction at the depths of 50–90 μm in 5 tissue samples.

Other information about the experimental materials, instrument, and methods are listed in detail in the ESI.†

Results and discussion

Optical properties and working mechanism of the probe

Investigation on the optical property of the probe shows that BNBD itself exhibits almost no fluorescence in a neutral solution (Fig. 1A) (Ex = 495 nm; Em = 560 nm). In contrast, when pH decreased to 1.98, BNBD showed a 150 fold enhancement in intensity (Fig. S4†), justifying the expected fluorescence turn on activated by H^+. Moreover, the highly acidic environment (pH < 2) kept the fluorescence intensity stable (Fig. S4†). Thus, the following experiments were performed in a buffer solution that could maintain the pH value at 1.98. Although the pH values in the stomach under a fasting condition (medically necessary condition) lies mainly in the range of 1–3,[43,44] while performing the analysis, the buffer would provide the pH value needed to obtain a stable signal. As a result, towards the added ClO^-/H_2S, BNBD exhibits remarkable fluorescence quenching at pH 1.98 but a negligible response under neutral condition (Fig. 1B and C). These properties demonstrate that the design for this H^+-activated dual-response probe is rational. However, a clear discrimination for ClO^- and H_2S is needed. According to our design (Scheme 1), the two analytes ClO^- and H_2S will bring about two corresponding products with the opposite electron push–pull, thus different absorbances (or colours) for the two products can be expected. Clearly, from Fig. 1D, the absorbance/colour of 300 nm/colourless and 400 nm/orange for ClO^- and H_2S, respectively, were observed. These behaviours can serve as the indicator for H_2S and ClO^- (Fig. S5†). To understand these optical phenomena, the mechanism of H^+-activated PET (photoinduced electron transfer) was estimated using the calculated orbital energy levels of the NBD fluorophore and reporting groups at the excited states (Scheme 1). Evidently in BNBD, the highest occupied molecule orbital (HOMO, −0.26232 hartree) of the donor (D_1) is high enough to cause efficient electron transfer to the HOMO (−0.33538 hartree) of the NBD fluorophore, thereby quenching the fluorescence. In the presence of H^+, a stable conjugated structure of phenyl–C=N^+ was formed with a rather low HOMO energy (−0.42964 hartree). Accordingly, PET from the phenyl–C=N^+ group to the NBD fluorophore was inhibited, thereby triggering strong fluorescence. Upon the addition of H_2S to H-BNBD,

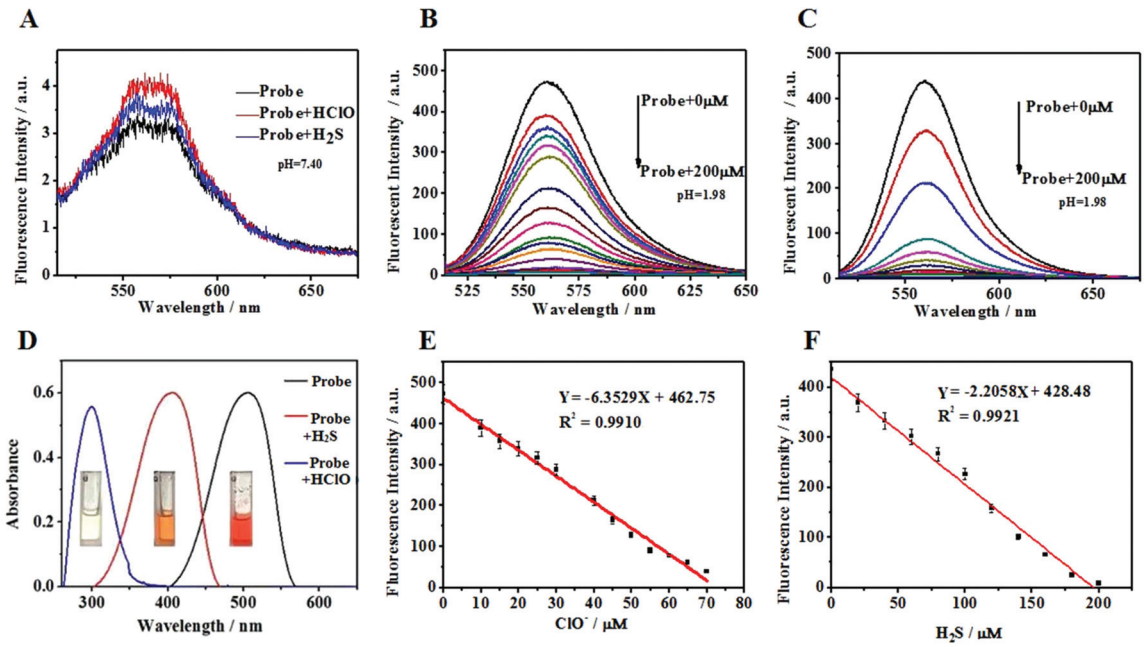

Fig. 1 The dependence of fluorescence intensity on ClO^- and H_2S, including (A) probe (3 μM), ClO^- (0.2 mM), H_2S (0.2 mM) and pH 1.98; (B) ClO^-: 0–200 μM; and (C) H_2S: 0–200 μM in the presence of the probe BNBD (3 μM). Investigation of the absorbance/colour response of the BNBD probe towards ClO^-/H_2S; (D) probe (3 μM), ClO^- (80 μM), H_2S (80 μM); linear relationships of BNBD probe to (E) ClO^- and (F) H_2S, established in simulated gastric juice (Ex = 495 nm; Em = 560 nm).

the nitro group of H-NBD (electron acceptor) was transformed into the amino group (electron donor) *via* reduction (characterized in Fig. S6, S7, and S16†), which drove the reverse PET from the fluorophore to the phenyl–C=N^+ group. Thus, the fluorescence quenching of BNBD was observed in response to H_2S in the presence of H^+. On the other hand, with the addition of ClO^- to H-BNBD, the C=N bond was oxidized to the –C=O group.[33] However, the oxidation products involving the nitrogen atom were not reported in previous literature. Considering that the intermediates are active and the products are difficult to isolate due to their similar polarity, we used an on-line mass spectrometer to monitor the various products including $-NH_2$ (D_2), –N=O (D_3), $-NO_2$ (D_4), and –NHOH (D_5) (Fig. S8†). As can be seen from Scheme 1, all the oxidation products have HOMOs (D_{1-5}) high enough to cause PET, which accounts for the quenching response of H-BNBD towards ClO^- in the presence of H^+. Thus, the novel H^+-activated probe with a controllable PET mechanism for fluorescence switching (Off–On–Off) proves to be rationally designed.

Optimization of the sensing conditions

Results show that 3.0 μM of BNBD is enough to exhibit a strong response for ClO^- or H_2S in the highly acidic environment (Fig. S9†), reflecting the high sensitivity of this probe. Phenomenally, it is the protonation that induces the large fluorescence enhancement, which can thereby be sensitively quenched by targets. In essence, the change in electron behaviour induced by the PET mechanism should be responsible for the sensitive responses. To perform the *in situ* quantification in biological samples, a fast response is requisite. Investigation on the response time shows that fluorescence reaches a constant intensity within quite a short time (50 s for ClO^- and 10 s for H_2S) (Fig. S10†). In fact, a chemical probe that can detect H_2S within 1 min is very rare to date.[45] The developed probe BNBD exhibits almost an instantaneous response to H_2S, which should be very suitable for biological studies. An important contribution to this rapid response may be that the high concentration of H^+ improves the oxidizing power of the nitro group. Therefore, the ultrafast response of BNBND in the presence of H^+ is particularly suitable for the *in situ* monitoring of the fluctuation of H_2S in stomach samples. In addition, the temperature-dependent responses of BNBD to ClO^-/H_2S were tested (Fig. S11†). Results show that the usual temperature, including the biological temperature (37 °C), is enough for this probe to display an ultrafast and strong response towards ClO^-/H_2S, which meets the requirement of biochemical analysis *in vivo* and *in vitro*.

Selectivity test

First, we examined the detection selectivity of BNBD for ClO^- and H_2S in parallel with ROS and RSS, respectively. As shown in Fig. 2, common ROS, including H_2O_2, $O_2^{\bullet-}$, $OH^\bullet$, $ONOO^-$, and NO_2^-, caused no obvious fluorescence response even at the concentration level of 300 fold over the target. Moreover, some potentially concomitant ions did not induce obvious interference. On the other hand, investigation of the BNBD probe towards H_2S indicates that common RSS (*i.e.*, GSH, CYS, GSNO, HSO_3^-, SO_3^{2-}, $S_2O_3^-$, $S_2O_4^{2-}$, and $S_2O_5^{2-}$) leads to a negligible response. Further investigation on the interferences from substances (amino acids and enzymes) normally co-existing in the stomach was performed, displaying their insignificant interference under the experimental conditions (Fig. 2). Thus, the developed probe proves to be specific to ClO^-/H_2S and insusceptible to other gastric contents. Since there is the possibility that ClO^- and H_2S are concomitant in the biological environment, an investigation on the response of BNBD to H_2S spiked by ClO^- was performed at the physiological concentration (Fig. S5†). As can be seen, with the increasing addition of ClO^- to H_2S, the fluorescence intensity does not decrease but increases, implying that the co-existing ClO^- will not cause an interfering fluorescence response to H_2S. With the continuous addition of ClO^-, the maximum and subsequent decrease was observed in the fluorescence intensity, representing the equivalent point and excessive ClO^-, respectively. These results should be attributable to the fast redox reaction between ClO^- with H_2S.[8] From this titration experiment, we can confirm that the remnant concentration of the lesser analyte should be rather low (< the detection limit). This low concentration is not enough to cause pathogenic damage to the stomach. Thus, only excess ClO- (or H_2S) will bring about significance for the pathogenic study. Therefore, in this study, the concomitant ClO^- and H_2S will not interfere with each other. Practically, the remnant H_2S or the excessive ClO^- can be easily identified by naked eyes with their distinct colour. These phenomena prompted us to investigate the UV absorbance behaviour in the simulated gastric juice. From Fig. S12,† we can see that no interference from the simulated gastric juice is observed, thereby ensuring the discrimination of ClO^-/H_2S. Consequently, with the developed probe, analytes, ClO^- and H_2S, as well as the homeostasis of ClO^-/H_2S can be selectively detected in the stomach samples.

Quantifications of ClO^-/H_2S and analytical strategy

Endogenous H_2S produced from the fast catabolism in organisms is rather low, thus sensitive detection is highly demanded. The quantification of H_2S and ClO^- was separately investigated. As can be seen from Fig. 1, linear relationships with the quite low detection limits of 2.7 nM and 6.9 nM were achieved for ClO^- and H_2S, respectively. Undoubtedly, the detection limit for H_2S with BNBD is comparable to the detection limit provided by the chemical probe reported as the most sensitive,[34] so was the detection limits for ClO^-.[46] We attributed this high detection sensitivity to both the large (150 fold) Off–On–Off switch of fluorescence and the strong oxidizing power of the nitro group and ClO^- under the acidic condition. Therefore, the BNBD probe shows the potential to quantify endogenous H_2S in acidic organisms.

Based on the abovementioned investigations, a quantitative analytical strategy for ClO^-/H_2S in acidic environment can be described as follows. First, the BNBD probe is spiked into enough B-R buffer to induce strong fluorescence; second,

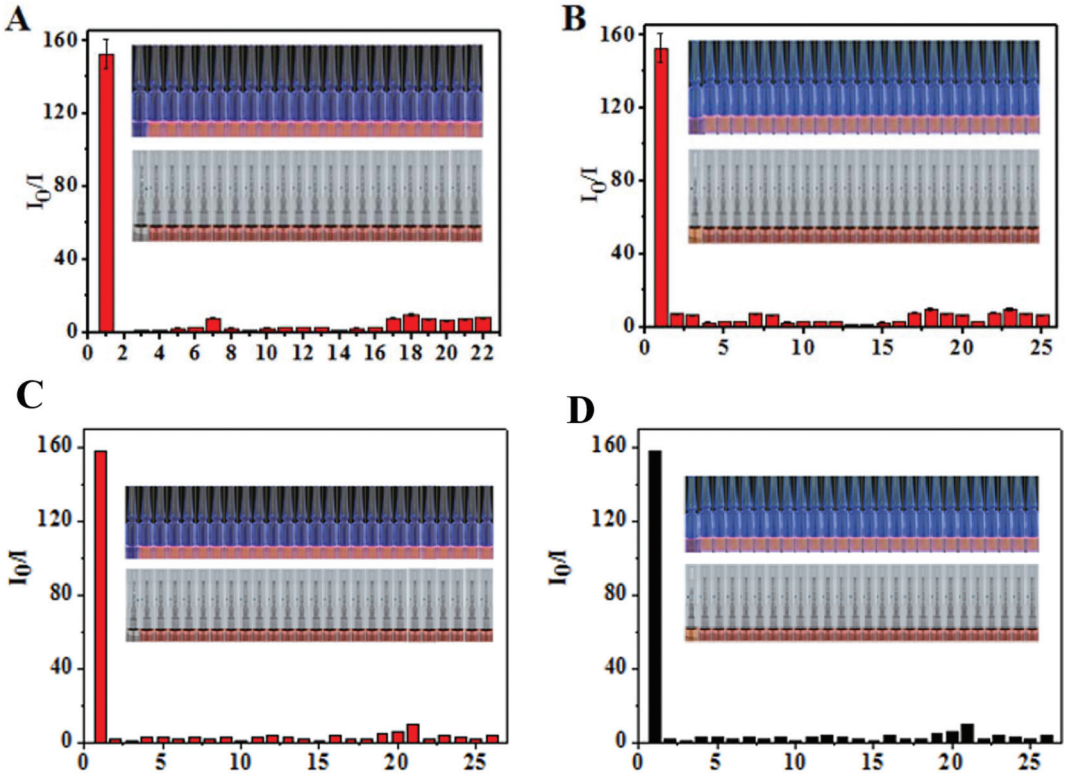

Fig. 2 Detection selectivity of the BNBD probe (3 μM) to ClO^-/H_2S investigated separately, including (A) 1, ClO^- (0.2 mM); 2, blank; 3, Cu^{2+} (10 mM); 4, Fe^{3+} (10 mM); 5, Zn^{2+} (10 mM); 6, Co^{2+} (10 mM); 7, Ca^{2+} (10 mM); 8, F^- (10 mM); 9, SO_4^{2-} (10 mM); 10, HCO_3^- (10 mM); 11, NO_2^- (10 mM); 12, NO_3^- (10 mM); 13, SO_3^{2-} (10 mM); 14, Cl^- (10 mM); 15, PO_4^{3-} (10 mM); 16, I^- (10 mM); 17, Mg^{2+} (10 mM); 18, hydrogen peroxide (60 mM); 19, superoxide (60 mM); 20, hydroxyl radicals (60 mM); 21, CH_3COOOH (60 mM); 22, and $ONOO^-$ (10 mM); (B) 1, H_2S (0.2 mM); 2, HSO_3^- (10 mM); 3, SO_3^{2-} (10 mM); 4, $S_2O_3^-$ (10 mM); 5, $S_2O_4^{2-}$ (10 mM); 6, $S_2O_5^{2-}$ (10 mM); 7, SCN^- (10 mM); 8, NO (10 mM); 9, H_2O_2 (10 mM); 10, superoxide (60 mM); 11, Cl^- (10 mM); 12, Br^- (10 mM); 13, I^- (10 mM); 14, N_3^- (10 mM); 15, NO_2^- (10 mM); 16, HCO_3^- (10 mM); 17, SO_4^{2-} (10 mM); 18, HPO_4^{2-} (10 mM); 19, OAc^- (10 mM); 20, citrate (10 mM); 21, lipoic acid (10 mM); 22, metallothionein (10 mM); 23, glutathione (10 mM); 24, cysteine (10 mM) and 25, *S*-nitrosoglutathione (10 mM). Pictures indicate the colour under ultraviolet and daylight; (C) 1, ClO^-; 2, alanine; 3, histidine; 4, methionine; 5, arginine; 6, glutamine; 7, isoleucine; 8, phenylalanine; 9, asparaginate; 10, leucine; 11, proline; 12, aspartic acid; 13, glycine; 14, lysine; 15, sarcosine; 16, serine; 17, threonine; 18, tryptophan; 19, valine; 20, glutamic acid; 21, cysteine; 22, lactate dehydrogenase; 23, aspartate aminotransferase; 24, glutamic-pyruvic transaminase; 25, alkaline phosphatase; 26, pepsin; and (D) 1, H_2S; 2, alanine; 3, histidine; 4, methionine; 5, arginine; 6, glutamine; 7, isoleucine; 8, phenylalanine; 9, asparaginate; 10, leucine; 11, proline; 12, aspartic acid; 13, glycine; 14, lysine; 15, sarcosine; 16, serine; 17, threonine; 18, tryptophan; 19, valine; 20, glutamic acid; 21, cysteine; 22, lactate dehydrogenase; 23, aspartate aminotransferase; 24, glutamic-pyruvic transaminase; 25, alkaline phosphatase and 26, pepsin. Pictures indicate the colour under ultraviolet and daylight (Ex = 495 nm; Em = 560 nm).

upon incubation with the sample, the absorbance/colour can indicate the specific target of H_2S or ClO^-; finally, the target is quantified with the quenching response of fluorescence. To evaluate this strategy, a series of simulated gastric juice (pH 2.1–5.1) spiked by Na_2S (40 μM) or ClO^- (40 μM) was prepared to serve as the quality control (QC) solutions. As shown in Fig. S13,† the fluorescence intensity in the QC solutions at different pH was observed to be approximately equal with slight errors, demonstrating that the pH fluctuation in the real samples would not interfere with the quantification using the proposed strategy. Based on these excellent properties and behaviours, this probe should be able to provide the accurate quantification of ClO^-/H_2S in real gastric samples.

Monitoring the homeostasis of ClO^-/H_2S in gastric Juice

The unique optical behaviour of the BNBD probe inspired us to develop its utility in stomach samples. Before performing analysis on gastric mucosa, it is necessary to carry out an analysis on the gastric juice. Note that the linear curves established in simulated and real gastric juice are comparable to those established in B-R buffer (Fig. S14†), demonstrating the robust applicability of BNBD with the developed strategy. Thus, we confirmed that this probe can be applied to quantify ClO^-/H_2S in real gastric juice without significant interference. On this basis, we applied BNBD to analyze samples of real gastric juice obtained from rabbits including a control group (intact), chlorinated group (control group fed with highly chlorinated water), and rehabilitation group (chlorinated group fed with L-Cys). As shown in Fig. 3a1, the remarkable colour of orange red indicates H_2S in the control group. The average content of H_2S in the gastric juice of the control group was 38.60 μM (±1.81 standard deviation). All the data were further validated by a commercial instrument for H_2S analysis (Fig. S17†). This result implies that H_2S exists in the gastric

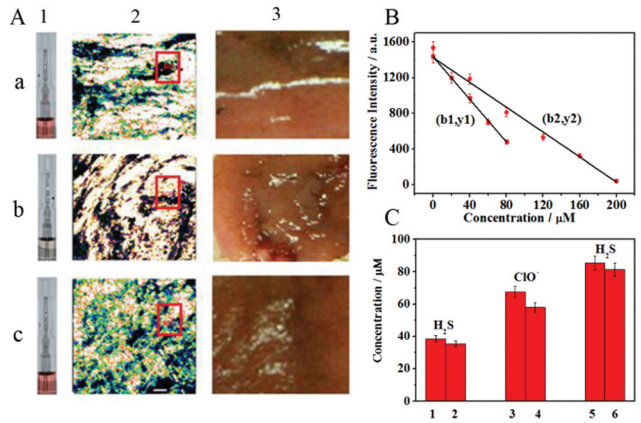

Fig. 3 Estimation of ClO^-/H_2S in stomach samples, including (A) images of BNBD-spiked gastric juice (1), pseudocolor images (scale bar: 20 μm) of gastric mucosa incubated with BNBD (3 μM) (2), images of the stomach lining (3), where a: control group, b: chlorinated group and (c) rehabilitation group; (B) the linear relationships for targets, ClO^- (b1/y1) and H_2S (b2/y2); and (C) the average contents of ClO^-/H_2S in gastric juice (1, 3, and 5) and mucosa (2, 4, and 6), where 1 and 2: control group, 3 and 4: chlorinated group, and 5 and 6: rehabilitation group (Ex = 488 nm; obtained: 500–600 nm).

juice of the intact rabbit as a protective substance under normal conditions. Then, analysis of the chlorinated group was carried out (Fig. 3b1). The sample showed a colourless state; thus, the content of ClO^- was obtained as 67.7 μM (±2.48) from the fluorescence intensity. Evidently, this result displays the accumulation of ClO^- in the gastric juice of the chlorinated group. The overwhelming excess of oxidative ClO^- in gastric juice is probably a pathogenic factor to the mucosa. Since H_2S has shown a curative effect on the stomach,[4,5] the rehabilitation group was prepared by the oral administration of L-Cys (a stimulus to increase H_2S) to the chlorinated group. As can be seen from Fig. 3c1, the indicative orange colour for H_2S reappeared and the average H_2S was estimated to be 85.42 μM (±2.81). Clearly, these results indicate that H_2S in the gastric juice of the rehabilitation group reached a high level and thus the curative effect of H_2S on the stomach could be expected. From these applications, it can be concluded that BNBD can be used to quantitatively monitor the existence and conversion of ClO^-/H_2S in the stomach media. However, the significance of this probe lies in not just the gastric juice but more in the tissue.

Quantifications of ClO^-/H_2S in mucosal tissue and monitoring of cross-talk between ClO^- and H_2S

Homeostasis of the ClO^-/H_2S pair plays a crucial role in stomach damage and repair. Therefore, long-term imbalance of ClO^-/H_2S may cause inflammation in the tissue. In the sense of etiology, if the inflammation can be associated with oxidative stress, the significance of quantification in inflammatory tissue should be great for the efficient diagnosis of stomach disease. From the aspect of tissue quantification, the *in situ* detection of ClO^- or H_2S is still challenging due to lack of satisfactory probes. To investigate the applicability of BNBD for *in situ* tissue quantification, the gastric mucosa samples obtained from the abovementioned control group, chlorinated group, and rehabilitation group were analysed. First of all, from the macroscopical assessment, the control group and chlorinated group showed normal and inflammatory states in the surface epithelium, respectively (Fig. 3a3 and b3). The congestive surface of the mucosa explains the fact that the accumulation of ClO^- by the intake of tap water leads to stomach discomfort.[47] Excitingly, alleviated inflammation of the mucosa was observed in the rehabilitation group (Fig. 3c3), which should be attributable to the curative effect of H_2S. These findings suggest the possible association between the pathologic manifestation and the *in situ* content of ClO^-/H_2S in the gastric mucosa. With the developed BNBD probe and analytical strategy, fluorescence confocal imaging of gastric mucosa was performed. From the pseudocolor images, an obvious difference in colour (reflecting the fluorescence intensity) between the chlorinated group (Fig. 3b2) and the other two groups (Fig. 3a2 and c2) can be observed, indicating ClO^- and H_2S present in the mucosa, respectively. Before tissue quantification, experiments to evaluate the photostability of the probe were carried out (Fig. S15†). First, in the region of interest (ROI), the fluorescence intensity of the BNBD probe remains stable within 30 min of monitoring in the mucosa. This result demonstrates that BNBD can emit consistently stable fluorescence and become immune to the mucosal tissue. Then, after being spiked by ClO^-/H_2S, the fluorescence intensity rapidly decreased to constant values, indicating that the photostability of remnant BNBD in the mucosa was also satisfactory under the experimental conditions. Therefore, the stable fluorescence signal obtained from the mucosa can be used to quantify ClO^-/H_2S with the proposed strategy. Based on the abovementioned validation, we applied the developed probe to *in situ* quantify ClO^-/H_2S in the gastric mucosa samples so as to evaluate the pathologic manifestation. The fluorescence intensity acquired from the 5 *xy* planes along the *z*-direction at the depths of 50–90 μm was obtained (Fig. 4 and Table 1). The linear curves for tissue quantification were established (Fig. 3B) with the calibrated ClO^-/H_2S in the gastric juice as variables, which is an important improvement to the accurate quantification in tissue reported before.[12] With the fluorescence intensity in ROI, the maximum contents of ClO^-/H_2S in the mucosa of the control group and chlorinated group are approximately 35.47 ± 2.64 μM (H_2S) and 57.91 ± 3.03 μM (ClO^-), respectively. These results indicated that the intake of chlorinated water can lead to the consumption of H_2S by the accumulated ClO^-. Since H_2S has an enhanced repair effect on tissue by the promotion of vasodilation and angiogenesis in mammals,[48] a deficiency of H_2S will cause local congestion in the mucosa. Moreover, excessive ClO^- can cause evident soft tissue necrosis[49] and mucosal injury from the cellular level to the surface,[50] which, in conjugation with H_2S deficiency, should be responsible for the observed inflammatory manifestation. In the rehabilitation group, by contrast, H_2S

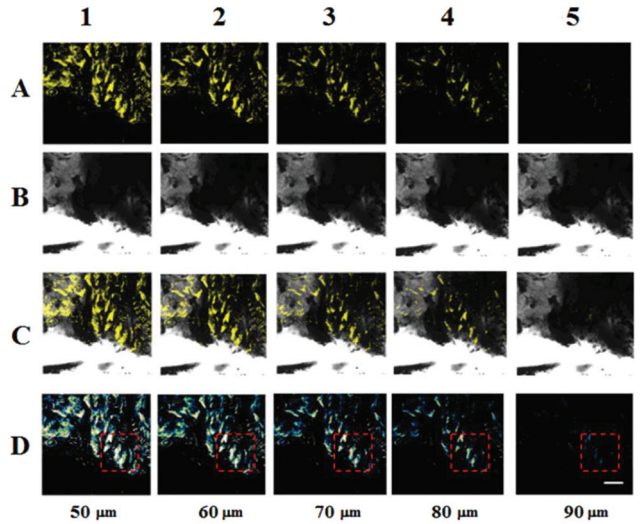

Fig. 4 Fluorescence confocal images of BNBD (3.0 μM)-labelled gastric mucosa incubated with Na_2S (20 μM), including (A) dark field, (B) bright field, (C) merged images by dark and bright fields and (D) pseudocolor images, where 1–5 are the respective images obtained along the *z*-direction in the range of 50–90 μm from the replicate experiments (n = 5), scale bar: 20 μm. Red box: region of interest (Ex = 488 nm; obtained: 500–600 nm).

Table 1 The fluorescence intensity of the selected ROI shown in Fig. 4 (n = 5)

Images Data Regions	1	2	3	4	5
ROI	1437	1200	972	701	482

reaches a relatively high level (81.12 ± 3.02 μM), suggesting that the homeostasis of ClO^-/H_2S in the gastric mucosa can be mediated by the intake of the stimulus. Together with the alleviated inflammatory manifestation observed in the rehabilitation group, this result leads us to believe that an oral H_2S-releasing drug will probably exert both the protective and the curative effects against gastritis by not only consuming the ROS but also promoting angiogenesis, respectively.[51] Based on the abovementioned findings, the shifting of the ClO^-/H_2S equilibrium in gastric mucosa can be monitored by the developed probe, providing the results closely with associated the pathologic manifestation, as well as the damaging effect of ClO^- and the therapeutic effect of H_2S on the mucosa. Although stomach diseases involve a complicated pathological process, an auxiliary diagnosis of gastritis caused by the imbalance of ClO^-/H_2S or deficiency of H_2S as a result of oxidative stress can be realized with the application of this probe. Overall, the *in situ* quantitative monitoring of ClO^-/H_2S homeostasis in acidic tissue was enabled; thus, useful information can be obtained for medical research on oxidative stress-caused gastritis.

Conclusions

In summary, we developed an ultrafast and ultrasensitive probe, BNBD, functioning *via* a novel H^+-activated mechanism for the *in situ* quantification of ClO^-/H_2S in acidic gastric tissue. The H^+-activated BNBD first undergoes the controllable PET process, switching the fluorescence from OFF to ON, and then the SEPP process, changing the behaviour of push–pull with the fluorescence quenched as a response to target. The resultant absorbance/colour and the fluorescence response serve to discriminate and quantify ClO^-/H_2S without interference. An analytical strategy for ClO^-/H_2S in acidic environment was devised, enabling the *in situ* quantification of endogenous H_2S and ClO^- in both gastric juice and mucosa with the fluorescence imaging technique for the first time. Particularly, the homeostasis of ClO^-/H_2S in mucosa was monitored and correlated well with the observed pathologic manifestation, which confirms the damaging/curative effects of ClO^-/H_2S. We, therefore, envision that the rationally designed probe BNBD will find extensive application in monitoring oxidative stress in the stomach, serving as an effective tool for the study of ClO^-/H_2S-related gastritis and drugs.

Acknowledgements

This work was supported by the National Natural Science Foundation of China (No. 21475074, 21403123, 21375075, 31301595, 21402106, 21475075, 21275089, 21405093, 21405094, 81303179, 21305076), the Taishan Scholar Foundation of Shandong Province, P. R. China, the Open Funds of the Shandong Province Key Laboratory of Detection Technology for Tumor Markers (KLDTTM2015-6), the Province Higher Educational Science and Technology Program (No. J14LC17), the Opening Foundation of Shandong Provincial Key Laboratory of Detection Technology for Tumor Makers (KLDTTM2015-9), and the China Postdoctoral Science Foundation (2016 M600531).

References

1 C.-H. Chang and E. L. Pearce, *Nat. Immunol.*, 2016, **17**, 364–368.
2 M. Radman, *DNA Repair*, 2016, 186–192.
3 K. Tokuda, K. Kida, E. Marutani, E. Crimi, M. Bougaki, A. Khatri, H. Kimura and F. Ichinose, *Antioxid. Redox Signaling*, 2012, **17**, 11–21.
4 R. Wang, *Antioxid. Redox Signaling*, 2010, **12**, 1061–1064.
5 J. L. Wallace and R. Wang, *Nat. Rev. Drug Discovery*, 2015, **14**, 329–345.
6 W. Hueper, *Ann. N. Y. Acad. Sci.*, 1963, **108**, 963–1038.
7 M. Whiteman, N. S. Cheung, Y.-Z. Zhu, S. H. Chu, J. L. Siau, B. S. Wong, J. S. Armstrong and P. K. Moore, *Biochem. Biophys. Res. Commun.*, 2005, **326**, 794–798.
8 P. Nagy and C. C. Winterbourn, *Chem. Res. Toxicol.*, 2010, **23**, 1541–1543.

9 Z. Shen, W. Wu and S. L. Hazen, *Biochemistry*, 2000, **39**, 5474–5482.
10 S. Ohnishi, M. Murata and S. Kawanishi, *Cancer Lett.*, 2002, **178**, 37–42.
11 J. Cui, L. Liu, J. Zou, W. Qiao, H. Liu, Y. Qi and C. Yan, *Exp. Ther. Med.*, 2013, **5**, 689–694.
12 H. J. Park, C. S. Lim, E. S. Kim, J. H. Han, T. H. Lee, H. J. Chun and B. R. Cho, *Angew. Chem., Int. Ed.*, 2012, **51**, 2673–2676.
13 J. Woolley, J. Stanicka and T. Cotter, *Trends Biochem. Sci.*, 2013, **38**, 556–565.
14 X. Li, X. Gao, W. Shi and H. Ma, *Chem. Rev.*, 2013, **114**, 590–659.
15 Q. Xu, C. H. Heo, G. Kim, H. W. Lee, H. M. Kim and J. Yoon, *Angew. Chem., Int. Ed.*, 2015, **54**, 4890–4894.
16 H. Xiao, K. Xin, H. Dou, G. Yin, Y. Quan and R. Wang, *Chem. Commun.*, 2014, **51**, 1442.
17 X. Chen, K. A. Lee, X. Ren, J. C. Ryu, G. Kim, J. H. Ryu, W. J. Lee and J. Yoon, *Nat. Protoc.*, 2016, **11**, 1219–1228.
18 Q. Xu, C. H. Heo, A. K. Jin, H. S. Lee, H. Ying, D. Kim, G. Kim, S. J. Nam and H. M. Kim, *Anal. Chem.*, 2016, **88**, 6615–6620.
19 V. S. Lin, W. Chen, M. Xian and C. J. Chang, *Chem. Soc. Rev.*, 2015, **44**, 4596–4618.
20 W. Chen, A. Pacheco, Y. Takano, J. J. Day, K. Hanaoka and M. Xian, *Angew. Chem., Int. Ed.*, 2016, **55**, 9993–9996.
21 Cao, W. Lin, K. Zheng and L. He, *Chem. Commun.*, 2012, **48**, 10529–10531.
22 C. S. Park, T. H. Ha, S. A. Choi, D. N. Nguyen, S. Noh, O. S. Kwon, C. S. Lee and H. Yoon, *Biosens. Bioelectron.*, 2016, 919–926.
23 M. Ren, B. Deng, X. Kong, K. Zhou, K. Liu, G. Xu and W. Lin, *Chem. Commun.*, 2016, **52**, 6415–6418.
24 H. Zhang, X. Kong, Y. Tang and W. Lin, *ACS Appl. Mater. Interfaces*, 2016, **8**, 16227–16239.
25 C. G. Dai, X. L. Liu, X. J. Du, Y. Zhang and Q. H. Song, *ACS Sens.*, 2016, **1**(7), 888–895.
26 L. Zhang, X. E. Zheng, F. Zou, Y. Shang, W. Meng, E. Lai, Z. Xu, Y. Liu and J. Zhao, *Sci. Rep.*, 2016, **6**, 18868.
27 Y. Huang, F. Yu, J. Wang and L. Chen, *Anal. Chem.*, 2016, 4122–4129.
28 F. Yu, M. Gao, M. Li and L. Chen, *Biomaterials*, 2015, **63**, 93–101.
29 F. Yu, P. Li, B. Wang and K. Han, *J. Am. Chem. Soc.*, 2013, **135**, 7674–7680.
30 L. Yi, L. Wei, R. Wang, C. Zhang, J. Zhang, T. Tan and Z. Xi, *Chem. – Eur. J.*, 2015, **21**, 15167–15172.
31 B. Wang, P. Li, F. Yu, J. Chen, Z. Qu and K. Han, *Chem. Commun.*, 2013, **49**, 5790–5792.
32 B. Wang, P. Li, F. Yu, P. Song, X. Sun, S. Yang, Z. Lou and K. Han, *Chem. Commun.*, 2013, **49**, 1014–1016.
33 L. Yuan, W. Lin, J. Song and Y. Yang, *Chem. Commun.*, 2011, **47**, 12691–12693.
34 X. Wang, J. Sun, W. Zhang, X. Ma, J. Lv and B. Tang, *Chem. Sci.*, 2013, **4**, 2551–2556.
35 Q. Fang, *Chem. Commun.*, 2012, **48**, 4767–4769.
36 H. R. Ellis and L. B. Poole, *Biochemistry*, 1998, **36**, 15013–15021.
37 K. Setsukinai, Y. Urano, K. Kakinuma, H. J. Majima and T. Nagano, *J. Biol. Chem.*, 2003, **278**, 3170–3175.
38 F. Auchère, G. Bertho, I. Artaud, J. P. Girault and C. Capeillère-Blandin, *Eur. J. Biochem.*, 2001, **268**, 2889–2895.
39 P. Zhang, J. Li, B. Li, J. Xu, F. Zeng, J. Lv and S. Wu, *Chem. Commun.*, 2015, **51**, 4414–4416.
40 M. U. Rao and W. A. Pryor, *Anal. Biochem.*, 1996, **236**, 242–249.
41 M. R. Corbo, A. Bevilacqua, M. Gallo, B. Speranza and M. Sinigaglia, *Innovative Food Sci. Emerging Technol.*, 2013, **18**, 196–201.
42 T. Teorell, *J. Gen. Physiol.*, 1939, **23**, 263–274.
43 M. Efentakis and J. Dressman, *Eur. J. Drug Metab. Pharmacokinet.*, 1998, **23**, 97–102.
44 J. Fletcher, A. Wirz, J. Young, R. Vallance and K. E. McColl, *Gastroenterology*, 2001, **121**, 775–783.
45 X. Feng, T. Zhang, J.-T. Liu, J.-Y. Miao and B.-X. Zhao, *Chem. Commun.*, 2016, **52**, 3131–3134.
46 H. Zhu, J. Fan, J. Wang, H. Mu and X. Peng, *J. Am. Chem. Soc.*, 2014, **136**, 12820–12823.
47 J. Zhang and X. Yang, *Analyst*, 2013, **138**, 434–437.
48 S. Fiorucci, E. Antonelli, E. Distrutti, G. Rizzo, A. Mencarelli, S. Orlandi, R. Zanardo, B. Renga, M. D. Sante and A. Morelli, *Gastroenterology*, 2005, **129**, 1210–1224.
49 U. K. Gursoy, V. Bostancı and H. H. Kosger, *Int. Endod. J.*, 2006, **39**, 157–161.
50 H. Dekigai, M. Murakami and T. Kita, *Dig. Dis. Sci.*, 1995, **40**, 1332–1339.
51 J. L. Wallace, *Dig. Dis. Sci.*, 2012, **57**, 1432–1434.